SAND2019-0318C

Radiometric calibration of range-Doppler radar data

A. W. Doerry*

Sandia National Laboratories, P.O. Box 5800, MS 0519, Albuquerque, NM 87185

ABSTRACT

We generally desire to relate radar data values to the Radar Cross Section (RCS) of a radar target echo. This is essential to selecting proper gain values in a radar receiver, maintaining dynamic range, and to properly interpret the resulting data and data products. Ultimately, this impacts proper radar design. We offer herein a basic analysis of relevant concepts and calculations to properly calibrate a monostatic radar's echoes with respect to RCS, and to select appropriate receiver gain values.

Keywords: radar; calibration; cross-section; RCS

1 INTRODUCTION

We concern ourselves in this paper with a radar system that interrogates a target and coherently processes the resulting echo data with the intent on quantifying the reflectivity of the target; its Radar Cross Section (RCS). Such systems include Synthetic Aperture Radar (SAR) and Moving Target Indication (MTI) radar systems, and similar systems. It its simplest form, this is illustrated in Figure 1 where σ is the target's RCS.

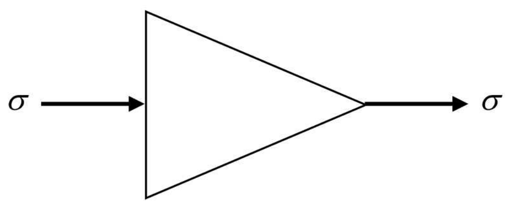

Figure 1. Basic model for radar measuring RCS.

The radar itself can be subdivided into major blocks, or subsections as shown in Figure 2.

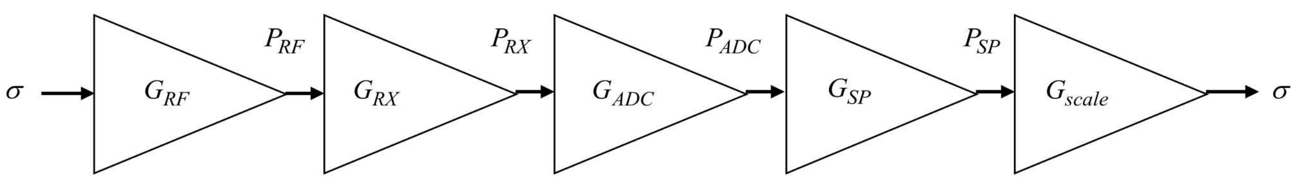

Figure 2. Basic system gain model.

Individual parameters are described as

---

* awdoerr@sandia.gov; phone 505-845-8165; www.sandia.gov/radar

Sandia National Laboratories is a multimission laboratory managed and operated by National Technology & Engineering Solutions of Sandia, LLC, a wholly owned subsidiary of Honeywell International Inc., for the U.S. Department of Energy's National Nuclear Security Administration under contract DE-NA0003525.

G_{RF} = RF channel gain, the conversion of target RCS to received (RX) power at the antenna port,
G_{RX} = Analog RX gain, the gain from antenna to input of the Analog to Digital Converter (ADC),
G_{ADC} = ADC conversion gain, to power relative to the square of the value of the Least Significant Bit (LSB),
G_{SP} = Signal Processing signal power gain,
G_{scale} = power scaling factor to achieve calibrated data. (1)

Gains are the ratio of output power to input power, hence positive real values. We stipulate that

$$G_{RF}G_{RX}G_{ADC}G_{SP}G_{scale} = 1. \tag{2}$$

We further identify specific power levels for a given RCS as

P_{RF} = received power from σ at the antenna port during a pulse echo,
P_{RX} = signal power presented to the ADC input during a pulse echo,
P_{ADC} = power at the ADC output during a pulse echo,
P_{SP} = power in the data product prior to any interpretive or calibration scaling. (3)

For digital data, power is simply the square of the data or pixel magnitude value.

For the remainder of this paper, for convenience, we will assume a pulse-Doppler radar, with constant-modulus pulse envelope, and monostatic corporate-fed antenna. Much of the subsequent analysis applies to other systems, too, but perhaps with slight modifications which we will not address. We will also use the term "image" to refer to the range-Doppler map resulting from processing the data, regardless of the actual radar mode employed.

2 INDIVIDUAL GAIN FACTORS

We examine the individual gain blocks.

2.1 RF Channel Gain

We develop here the relationship between the target RCS and the power at an antenna port. Consistent with an earlier report,[1] we identify the radar equation that governs this relationship as

$$P_{RF} = \frac{P_{TX} G_{A,c}^2 \lambda^2 \sigma}{(4\pi)^3 r_c^4 L_{TX} L_{radome} L_{atmos,c}}, \tag{4}$$

where

P_{TX} = Transmit (TX) power in Watts during the pulse,
$G_{A,c}$ = one-way antenna gain towards image center, typically assumed to be the reference location or direction,
λ = nominal wavelength in meters,
r_c = nominal range to image center in meters,
L_{TX} = loss from power amplifier to antenna port,
L_{radome} = 2-way loss through radome, and
$L_{atmos,c}$ = 2-way atmospheric loss to image center. (5)

The subscript 'c' denotes the image center. For targets away from the image center, range-dependent losses and antenna pattern gain variations need to be accommodated. We discuss in more detail this later. From Eq. (4) we identify

$$G_{RF} = \frac{P_{RF}}{\sigma} = \frac{P_{TX} G_{A,c}^2 \lambda^2}{(4\pi)^3 r_c^4 L_{TX} L_{radome} L_{atmos,c}} . \tag{6}$$

Strictly speaking, for a target scene of any significant size, the antenna gain will not be constant over the scene, but exhibit antenna beam-pattern effects; attenuations away from its boresight direction. In addition, range-dependent variations across the scene will also become apparent in the signal echo power. These combine to render G_{RF} as spatially variant across the target scene, ultimately manifesting as uneven shading in the range-Doppler image. This can be compensated in the signal processing, but at the expense of some other data characteristics, to be addressed later.

2.2 Analog Receiver (RX) Gain

The analog RX gain is often somewhat adjustable, and generally must be calibrated. Because the ADC is often somewhat of a dynamic range choke-point, the specific gain is typically selected to accommodate several criteria, often conflicting. This requires an understanding of the ADC characteristics, which we now briefly address.

We identify the following relevant ADC parameters

$V_{ADC,fs}$ = ADC full scale input voltage range of ADC,

b_{ADC} = actual number of bits in ADC output, and

R_{ADC} = impedance at ADC input, across which the voltage is developed. (7)

The nominal quantization voltage for the ADC is based on the number of bits, and is calculated as

$$V_q = \frac{V_{ADC,fs}}{2^{b_{ADC}}} . \tag{8}$$

2.2.1 System Noise

The system noise is usually referenced to the front-end of the receiver,[2] and often termed "receiver noise." We identify this noise level at the ADC input as

$$N_{RX} = kT_{ref} B_N F_{N,A} G_{RX} , \tag{9}$$

where

k = Boltzmann's Constant = 1.3806504 x 10^{-23} J/K,

T_{ref} = reference temperature = 290 K,

B_{IFA} = analog noise/data bandwidth at the ADC input, and

$F_{N,A}$ = analog noise factor (also called noise figure, especially when given in units of dB). (10)

The analog noise factor is the noise factor due to all components "prior" to the ADC, and does not include the quantization noise added by the ADC conversion process or any subsequent processing. Noise can be useful for dithering an input signal, and to help mitigate effects of ADC nonlinearities, but too much noise will limit dynamic range. Consequently, we desire to limit gain such that

$$G_{RX} \le \frac{K_{noise}^2 \left(V_q^2 / R_{ADC} \right)}{kT_{ref} B_{IFA} F_{N,A}} , \tag{11}$$

where

K_{noise} = desired noise amplification with respect to a quantization step. (12)

We typically desire maximum gain for $K_{noise} \approx 1$, but, as previously stated, there are reasons for somewhat more noise, yet.[3,4] However, for a sufficiently complex target set (e.g. lots of distributed clutter), sufficient dithering will often occur even for actual system noise manifesting substantially below the ADC quantization level. Other options also are available for system designs, such as out-of-band noise dithering.

2.2.2 Bright Distributed Clutter

We will make the typical and adequate assumption that the clutter statistics in the scene being interrogated by the radar are Gaussian, with reflectivity given as

$\sigma_{1,ref}$ = maximum expected clutter reflectivity of distributed clutter. (13)

Nominal land clutter levels are discussed in numerous sources in the literature, including a text by Ulaby and Dobson,[5] with brighter urban clutter discussed in a paper by Raynal, et al.[6] A reasonable value for bright clutter reflectivity might be 0 dBsm/m^2 at Ku-band. This normalized clutter reflectivity integrates in the radar to yield an overall RCS, and hence clutter power, to the ADC, where we calculate this as

$$P_{ADC,clutter,\max} = \frac{P_T G_A^2 \lambda^2 \sigma_{H,\max,ref} G_{RX}}{(4\pi)^3 r_c^4 L_{TX} L_{radome} L_{atmos,c}}, \tag{14}$$

where we define

$\sigma_{H,\max,ref}$ = the net RCS of the distributed clutter power impinging upon the ADC. (15)

The issue now becomes relating clutter reflectivity $\sigma_{1,ref}$ to net clutter RCS seen by the ADC $\sigma_{H,\max,ref}$.

Presuming correlation processing for range compression, the net RCS of a clutter scene with this reflectivity that makes it to the ADC input will be approximated as

$$\sigma_{H,\max,ref} \le \sigma_{1,ref} \left(\frac{r_c \tan(\theta_{az})(c/2) T_{TX}}{\cos(\psi_{g,c})} \right) \tag{16}$$

where

θ_{az} = nominal azimuth beamwidth of the antenna,
T_{TX} = the transmitted pulsewidth,
c = velocity of propagation, and
$\psi_{g,c}$ = nominal grazing angle at swath center. (17)

If stretch processing[7] is used, then the RCS of a clutter scene is limited by range-swath width that makes it to the ADC input, namely

$$\sigma_{H,\max,ref} \le \sigma_{1,ref} \left(\frac{r_c \tan(\theta_{az}) D_r}{\cos(\psi_{g,c})} \right), \tag{18}$$

where

$$D_r = \text{range swath present in the analog signal at the ADC input.} \tag{19}$$

We note that for stretch processing, which typically assumes a LFM chirp waveform is used, the range swath width D_r is typically dependent on the bandwidth at the ADC as

$$D_r = \frac{\pi c B_{IFA}}{\gamma_0}, \tag{20}$$

where we identify

$$\gamma_0 = \text{the nominal LFM chirp rate in rad/s/s.} \tag{21}$$

Another limit depends on the antenna illumination of the target scene due to the antenna elevation beamwidth, namely

$$\sigma_{H,\max,ref} \le \sigma_{1,ref} \left(\frac{r_c^2 \tan(\theta_{az}) \tan(\theta_{el})}{\sin(\psi_{g,c})} \right), \tag{22}$$

where

$$\theta_{el} = \text{nominal elevation beamwidth of the antenna.} \tag{23}$$

Consequently, the clutter power at the ADC is Eq. (14) limited by the lesser of Eq. (18) or Eq. (16), whichever is applicable, and Eq. (22). Because the clutter is presumed to be statistically Gaussian, the RMS clutter value needs to be a fraction of the maximum allowable power level into the DRX input, by several standard deviations. This power margin factor is typically about 16, for a 12-dB margin, or two bits. Therefore, we require

$$P_{ADC,clutter,\max} \le \frac{1}{M_{ADC,clutter}} \left(\frac{V_{ADC,fs}^2}{4R_{ADC}} \right), \tag{24}$$

where

$$M_{ADC,clutter} = \text{power margin factor for clutter.} \tag{25}$$

This, in turn, places another limit on analog RX gain due to distributed clutter as

$$G_{RX} \le \frac{(4\pi)^3 r_c^4 L_{TX} L_{radome} L_{atmos,c}}{M_{ADC,clutter} P_T G_A^2 \lambda^2 \sigma_{H,\max,ref}} \left(\frac{V_{ADC,fs}^2}{4R_{ADC}} \right). \tag{26}$$

2.2.3 Bright Discrete Clutter

Clutter may also contain discrete scatterers, sometimes quite bright; with relatively strong RCS. Receiver gain needs to accommodate some degree of bright clutter discretes. Accordingly, we define the maximum clutter discrete RCS as

$$\sigma_{D,\max,ref} = \text{maximum clutter discrete RCS expected.} \tag{27}$$

The maximum total clutter power at the ADC input due to a clutter discrete is then calculated to be

$$P_{ADC,discrete,\max} = \frac{P_T G_A^2 \lambda^2 \sigma_{D,\max,ref} G_{RX}}{(4\pi)^3 r_c^4 L_{TX} L_{radome} L_{atmos,c}} . \tag{28}$$

We stipulate the maximum allowable discrete signal level at the ADC input needs to be limited to

$$P_{ADC,discrete,\max} \le \frac{1}{M_{ADC,discrete}} \left(\frac{V_{ADC,fs}^2}{4R_{ADC}} \right), \tag{29}$$

where

$$M_{ADC,discrete} = \text{power margin factor for a maximum discrete clutter RCS.} \tag{30}$$

Since we are dealing with a discrete scatterer, the RMS target value needs to be somewhat lower than the maximum allowable power level into the ADC input. This power margin factor needs to be at least 3 dB for a sinusoidal signal. This, in turn, places another limit on analog RX gain due to a clutter discrete as

$$G_{RX} \le \frac{(4\pi)^3 r_c^4 L_{TX} L_{radome} L_{atmos,c}}{M_{ADC,discrete} P_T G_A^2 \lambda^2 \sigma_{D,\max,ref}} \left(\frac{{V_{ADC,fs}}^2}{4R_{ADC}} \right). \tag{31}$$

2.2.4 Maximum Target RCS

We now define a maximum target RCS that which we wish pass through the ADC as

$$\sigma_{T,\max,ref} = \text{maximum target RCS expected.} \tag{32}$$

The maximum target echo power at the ADC input is then calculated to be

$$P_{ADC,target,\max} = \frac{P_T G_A^2 \lambda^2 \sigma_{T,\max,ref} G_{RX}}{(4\pi)^3 r_c^4 L_{TX} L_{radome} L_{atmos,c}} . \tag{33}$$

However, the maximum allowable target signal level at the ADC input is limited to

$$P_{ADC,target,\max} \le \frac{1}{M_{ADC,target}} \left(\frac{V_{ADC,fs}^2}{4R_{ADC}} \right), \tag{34}$$

where

$$M_{ADC,target} = \text{power margin factor for a maximum target RCS.} \tag{35}$$

Since a target is typically a discrete scatterer, the RMS target value needs to be somewhat lower than the maximum allowable power level into the ADC input. This power margin factor needs to be at least 3 dB for a sinusoidal signal. This, in turn, places another limit on analog RX gain due to a target as

$$G_{RX} \le \frac{(4\pi)^3 r_c^4 L_{TX} L_{radome} L_{atmos,c}}{M_{ADC,target} P_T G_A^2 \lambda^2 \sigma_{T,\max,ref}} \left(\frac{{V_{ADC,fs}}^2}{4R_{ADC}} \right). \tag{36}$$

2.2.5 Final Analog RX Gain Selection and Comments

The actual analog RX gain needs to accommodate all of the limits previously discussed. That is, the final G_{RX} needs to be the lesser of Eq. (11), Eq. (26), Eq. (31), and Eq. (36). Furthermore, the actual gain G_{RX} might need to be selected from some limited set of values available to the radar, due to specific discrete attenuator settings.

Furthermore, we are ignoring any notions of Automatic Gain Control (AGC) or Sensitivity Time Control (STC). We state without elaboration that these functions, while affording utility in dynamic range management, nevertheless often substantially complicate radiometric calibration of radar data.

While a number of approximations have been used to calculate gain limits, these are all meant to provide appropriate margins for proper dynamic range management. Once the analog RX gain has been selected, it is a fixed value, and the approximations no longer have an overt effect beyond perhaps slight variations in the operating margins.

Finally, we stipulate that the radar receiver needs to remain acceptably linear over all anticipated analog RX gain values, for maximum amplitude signals at the ADC input. This becomes a fundamental design criterion.

2.3 ADC Conversion Gain

Consider an input signal with RMS magnitude equal to the LSB quantization step-size. After ADC conversion, this will yield a sampled and quantized data value with unit RMS value. This allows us to identify

$$G_{ADC} = \frac{1}{\left(V_q^2 / R_{ADC}\right)} = \frac{R_{ADC}}{V_q^2} . \tag{37}$$

We offer here a brief comment on the ADC input impedance R_{ADC}. We note that the analog RX gain limitations, and ultimately the definition of analog RX gain itself, are proportional to $1/R_{ADC}$, whereas the ADC conversion gain is proportional to R_{ADC}. This means that within the product $G_{RX} G_{ADC}$, the actual value for R_{ADC} is immaterial. Consequently, whether we use the actual input impedance, or some convenient reference value, ultimately has no effect on radiometric calibration of the radar. The caveat is that the same R_{ADC} is used in both gain factors.

2.4 Signal Processing Gain

Range-Doppler data/image processing is typically an attempt to implement a matched filter to a point target response, albeit often with some additional perturbations to mitigate processing sidelobes, such as the employment of window taper functions.[8] For modern radars, it is almost always coherent processing.

If we transmit a constant modulus signal, then we would expect its echo to also be constant modulus, albeit gain-adjusted by the various gains and losses of the radar system. If the echo is from a point target at some reference location in the target scene, then the signal processing will impart some gain to that echo signal level. The signal gain might be large, unity, or even fractional (representing a loss). If the echo signal amplitude at the ADC output (signal processor input) were unity, then the output processed signal's magnitude would represent an amplitude gain, and the square of the amplitude would represent the power gain for the reference signal.

For example, if the matched filter signal processing were a 2-dimensional Discrete Fourier Transform defined as

$$X(u,v) = \sum_{m=0}^{M-1} \sum_{n=0}^{N-1} x(m,n) e^{-j2\pi\left(\frac{mu}{M}+\frac{nv}{N}\right)} . \tag{38}$$

then the signal processing power gain would be

$$G_{SP} = (MN)^2 . \tag{39}$$

For many radar systems the reference location is the center of the range swath, also often the aim-point of the antenna, but all system gains ignore any frequency notches and similar artifacts. The signal processing gain also assumes a linear processor; assumes no clipping or rounding due to discrete/integer math.

It is also true that the signal processing may compensate for any known spatially-variant gain variations, including antenna beam-pattern gain variations, as well as range-dependent losses. The intent would be for the output of the signal processor to no longer exhibit any spatially-variant overall system gains. The price for this is that the background noise often becomes spatially variant as a byproduct of these signal corrections.

We further stipulate that there is no reason that additional uniform gains/losses can't be applied within the signal processor. In fact, there might be very good reasons for doing so.

Finally, we need to remain mindful that when quadrature demodulation and sampling is used, to create complex data, then there is often an implicit doubling of the signal power that needs to be counted in the overall signal processing gain, if not elsewhere.

2.5 RCS Scale Factor

To this point, we have defined the first four gains in Figure 2. We observe that all elements of Eq. (2) save one are defined. We now rearrange Eq. (2) to identify the calculation for G_{scale} as

$$G_{scale} = \frac{1}{G_{RF} G_{RX} G_{ADC} G_{SP}} . \tag{40}$$

In terms of a calibration scale factor for the data itself, we define the magnitude scaling factor as

$$C_{cal} = \sqrt{G_{scale}} = \frac{1}{\sqrt{G_{RF} G_{RX} G_{ADC} G_{SP}}} . \tag{41}$$

That is, multiplying each complex pixel value x in the image with C_{cal} will yield a calibrated range-Doppler map where

$$\sigma = \left| C_{cal}\, x \right|^2 . \tag{42}$$

2.6 Some Comments

Another dynamic range choke-point, especially for imaging radars, is the output image itself. This is because the output image is often represented with integer values for the pixels, sometimes complex-valued pixels. [9] This ultimately means that the radiometric calibration factor C_{cal} cannot be arbitrary, and furthermore might need to be some precise predetermined value to maximize the useable dynamic range of RCS values that can be represented. This means that the output data might need scaling in the signal processor itself, with the signal processing gain 'adjusted' to be

$$G_{SP} = \frac{1}{G_{RF} G_{RX} G_{ADC} G_{scale}} = \frac{1}{G_{RF} G_{RX} G_{ADC} C_{cal}^2} . \tag{43}$$

The bottom line is that various gain factors need to consider various dynamic range choke-points, often related to limited-precision integer values. A principal choke-point is the ADC input. A secondary choke-point for some radar systems is an integer-representation of the range-Doppler image.

3 RELATED ISSUES

We now discuss some related issues to RCS calibration.

3.1 Gain Accuracy and Precision

The accuracy and precision of a calculated RCS depends on the accuracy and precision of the various gain factors in Figure 1, and listed in Eq. (1).

The accuracy of RF channel gain G_{RF} depends on accurately knowing a number of radar parameters, as well as transmission properties along the path between radar and target scene. This requires, among other things, accurate calibration of transmitter power, antenna gain and beam pattern characteristics, and radar system losses. Particularly problematic, especially at long ranges for higher microwave frequencies, is accurate knowledge of atmospheric losses.

The accuracy of analog RX gain G_{RX} is a calibration issue, and will vary from radar to radar even for the same model, and like components, and can often be expected to further vary over temperature and with age. As with any radar, the calibration schedule will depend on the accuracy and precision required of the gain value, as well as the stability of a calibration measurement. We stipulate also that some other parameters, such as system noise factor, often depend on the specific gain setting of the radar, and also needs to be calibrated accordingly.

The ADC conversion gain G_{ADC} is typically fairly stable. Any minor fluctuations in this gain can also be rolled into measurements of analog RX gain G_{RX}.

One might expect Signal Processing gain G_{SP} to be essentially constant and stable, since it is a digital computation of data. Recall, however, that it attempts to implement a matched filter to the data it "expects." Its accuracy depends on the "goodness" of the matched filter to the actual data. If the data departs from what is expected, say, due to uncompensated motion measurement errors, or other system nonlinearities, then the matched filter won't be properly matched. In imaging radars this is otherwise known as misfocusing of the image, which also impacts peak values. Uncompensated range-walk is also an issue. Customarily, when focus is an issue, data-driven autofocus techniques are employed to enhance the matched filter performance.

3.2 Calibration

Calibration particularly of elements of RF channel gain G_{RF}, and of analog RX gain G_{RX}, is essential for accurate RCS measurements. The breadth of techniques, and the schedules under which they are employed, is beyond the scope of this paper. Nevertheless, we offer some rudimentary comments here anyway.

Common laboratory calibration techniques include the use of microwave/optical delay lines, and microwave anechoic chambers.

Common in-situ calibration techniques include the use of various on-board reference signals, including pilot tones, and even front-end thermal noise.

In-flight calibration and testing typically involves using known canonical reflectors of some sort.[10] This might even include radar transponders, where precise Doppler shifts can even be added to simulate target motion. Particularly difficult is proper accounting for atmospheric losses, especially at higher microwave frequencies. Effects of the atmosphere can be minimized at nearer ranges. At longer ranges, better models of the actual atmosphere can help, but accurate absolute measurements still remain problematic. This leaves us with relative RCS measurements.

Finally, while we have been tacitly discussing single-channel radar systems, we note that multi-channel radar systems have additional calibration requirements that require additional calibration measurement techniques.[11]

3.3 Noise Level in the ADC Data

In addition to having well calibrated signal data, it is also often quite useful to know the background noise level both at the ADC output, and in the final range-Doppler image. After sampling and quantization, and assuming adequate dithering of the ADC, the broadband noise power at the ADC output is identified as

$$N_{ADC} = kT_{ref} B_N F_{N,A} G_{RX} G_{ADC} + \frac{1}{12}. \tag{44}$$

The $1/12$ term is the variance due to quantization. Note that the ADC output noise power N_{ADC} is never less than that due to quantization noise. A minor note is that the first term is the variance of a Gaussian distribution, and the $1/12$ is the variance due to a uniform distribution. Nevertheless, after signal processing, which entails linear processing, by the Central Limit Theorem the noise at the signal processor output is effectively Gaussian in nature.

We also recall that the noise factor $F_{N,A}$ in Eq. (44) is the "analog" noise factor, representing the noise factor due to all components before the ADC. We may also write Eq. (44) as

$$N_{ADC} = \left(kT_{ref} B_N F_{N,A} G_{RX} G_{ADC} + \frac{1}{12} \right) = kT_{ref} B_N F_N G_{RX} G_{ADC}, \tag{45}$$

where

$$F_N = F_{N,A} + \frac{1}{12\, kT_{ref} B_N G_{RX} G_{ADC}} = \text{overall system noise factor.} \tag{46}$$

The overall system noise factor F_N incorporates the effects of quantization by the ADC. Note the trend that as the analog RX gain G_{RX} decreases, the system noise factor F_N increases.

A key point here is that for proper radar design, there is no single noise factor value to use. Noise factor values relative to different parts of the overall receiver need to be considered for different purposes. Furthermore, this analysis is about broadband noise power, and ignores any spurious signals and other narrow-band noise sources.

3.4 Noise Level in the Range-Doppler Image

The purpose of signal processing generally includes the enhancement of the Signal-to-Noise Ratio (SNR) of the input data. SNR is a ratio of powers or energies. Consequently, we expect that the signal power gain is generally greater than the noise power gain. Recall that the signal power gain is given as G_{SP}. Another important measure of the signal processing is the gain in SNR itself, which we define as

$$G_{SP,SNR} = \text{gain in SNR of the signal processing.} \tag{47}$$

Consequently, the noise power in the signal processor's output image is calculated as

$$N_{SP} = \frac{kT_{ref} B_N F_N G_{RX} G_{ADC} G_{SP}}{G_{SP,SNR}}. \tag{48}$$

This noise power level can be converted to a noise-equivalent RCS using G_{scale}.

We stipulate that the noise power of Eq. (48) does not include any multiplicative noise, such as effects of system nonlinearities, etc.

4 SUMMARY & CONCLUSIONS

We offer several summary comments.

- Radiometric calibration of a range-Doppler image requires knowledge of the various system gains.
- Precisely and accurately determining system gains is a function of calibration. Gain calibration is essential.
- A principal dynamic range choke-point is the ADC. Receiver analog gain selection needs to accommodate the ADC dynamic range limitations, with margins, as well as target and clutter levels reasonably expected.
- A secondary dynamic range choke-point is often the range-Doppler image itself, particularly when pixel values are represented with integers.
- Expected noise levels at the ADC output, as well as in the range-Doppler image, can be readily calculated.

ACKNOWLEDGEMENTS

Sandia National Laboratories is a multimission laboratory managed and operated by National Technology and Engineering Solutions of Sandia, LLC., a wholly owned subsidiary of Honeywell International, Inc., for the U.S. Department of Energy's National Nuclear Security Administration under contract DE-NA-0003525.

This paper describes objective technical results and analysis. Any subjective views or opinions that might be expressed in the paper do not necessarily represent the views of the U.S. Department of Energy or the United States Government.

REFERENCES

[1] Armin W. Doerry, *Performance Limits for Synthetic Aperture Radar – second edition*, Sandia National Laboratories Report SAND2006-0821, Unlimited Release, February 2006.

[2] Armin W. Doerry, *Noise and Noise Figure for Radar Receivers*, Sandia National Laboratories Report SAND2016-9649, Unlimited Release, October 2016.

[3] Armin W. Doerry, Dale F. Dubbert, Bert L. Tise, "Spurious effects of analog-to-digital conversion nonlinearities on radar range-Doppler maps," SPIE 2015 Defense & Security Symposium, Radar Sensor Technology XIX, Vol. 9461, Baltimore, MD, 20-24 April 2015.

[4] Armin W. Doerry, "Balancing I/Q data in radar range-Doppler images," SPIE 2015 Defense & Security Symposium, Radar Sensor Technology XIX, Vol. 9461, Baltimore, MD, 20-24 April 2015.

[5] Fawwaz T. Ulaby, M. Craig Dobson, *Handbook of Radar Scattering Statistics for Terrain*, ISBN-13: 978-0890063361, Artech House, 1989.

[6] Ann Marie Raynal, Douglas L. Bickel, Dale F. Dubbert, Tobias J. Verge, Bryan L. Burns, Ralf Dunkel, Armin W. Doerry, "Radar cross section statistics of cultural clutter at Ku-band", SPIE 2012 Defense, Security & Sensing Symposium, Radar Sensor Technology XVI, Vol. 8361, Baltimore, MD, 23-27 April 2012.

[7] William J. Caputi, Jr., "Stretch: A Time-Transformation Technique", *IEEE Transactions on Aerospace and Electronic Systems*, Vol. AES-7, No. 2, pp 269-278, March 1971.

[8] Armin W. Doerry, *Catalog of Window Taper Functions for Sidelobe Control*, Sandia National Laboratories Report SAND2017-4042, Unlimited Release, April 2017.

[9] A. W. Doerry, "Representing SAR complex image pixels," SPIE 2016 Defense & Security Symposium, Radar Sensor Technology XX, Vol. 9829, Baltimore, MD, 17-21 April 2016.

[10] Armin W. Doerry, *Reflectors for SAR Performance Testing – second edition*, Sandia National Laboratories Report SAND2014-0882, Unlimited Release, Supersedes SAND2008-0396, February 2014.

[11] D. L. Bickel, A. W. Doerry, "Measuring channel balance in multi-channel radar receivers," SPIE 2018 Defense & Security Symposium, Radar Sensor Technology XXII, Vol. 10633, Orlando, FL, 15-19 April 2018.